SCIENCE CHINA
Information Sciences

• RESEARCH PAPER •

February 2022, Vol. 65 122402:1–122402:11
https://doi.org/10.1007/s11432-020-3175-6

A non-contact flexible pyroelectric sensor for wireless physiological monitoring system

Jian HE[1†], Sen LI[1†], Xiaojuan HOU[1], Yongjun ZHOU[2], Hao LI[2], Min CUI[1], Tao GUO[1], Xiangdong WANG[3*], Jiliang MU[1], Wenping GENG[1] & Xiujian CHOU[1*]

[1]*Science and Technology on Electronic Test and Measurement Laboratory, North University of China, Taiyuan* 030051*, China;*
[2]*Science and Technology on Near-Surface Detection Laboratory, Wuxi* 214035*, China;*
[3]*China Institute of Sport Science, Beijing* 100061*, China*

Received 7 July 2020/Revised 28 October 2020/Accepted 25 January 2021/Published online 14 December 2021

Abstract Recently, human physiological information wireless monitoring in real-time is particularly important in health analysis. As a solution, a non-contact wireless physiological monitoring system based on pyroelectric generator (PyG), whose core part consists of a wireless circuit processing module and a polyvinylidene fluoride (PVDF) film, has been successfully designed. Owing to the temperature change under the stimulation of an external heat source, the output voltage of the PyG self-powered flexible sensor increases with the heat source temperature variation in the range of 295–355 K. Furthermore, based on the natural temperature oscillation between the living body and surrounding environment, the sensor can realize human physiological information assessment, for example, temperature monitoring of the palms, fingers, respiratory heat signals from mouth or nose or non-contact spatial heat mapping recognition of finger movement via sensor array. On this basis, a portable wireless monitoring system was designed by integrating the intelligent sensor with a signal conditioning circuit, data conversion storage module, Bluetooth module, and power module. This system can acquire real-time human oral or nasal breathing signals in the personal mobile app to evaluate the physiological state of individuals. Additionally, the wireless monitoring system can be activated within 10 m, demonstrating the application of PyG sensors in remote data transmission.

Keywords non-contact, pyroelectric generator, human body heat, environmental thermal energy, wireless monitoring system

Citation He J, Li S, Hou X J, et al. A non-contact flexible pyroelectric sensor for wireless physiological monitoring system. Sci China Inf Sci, 2022, 65(2): 122402, https://doi.org/10.1007/s11432-020-3175-6

1 Introduction

With the development of artificial intelligence technology [1–3], the pursuit of lighter and smarter mobile medical systems has drawn great interests. Among them, the intelligent electronic monitoring equipment is one of the most significant advancements [4,5]. Compared with conventional medical systems, wireless sensing circuits combined with advanced flexible electronics are changing traditional diagnostic methods and endowing medical devices with portable [6–9], remote [10] and real-time [11,12] monitoring functions. Specifically skin temperature [13, 14] and respiratory frequency [15] are key indicators for evaluating human health. Therefore, the design and development of wireless sensor circuits [16] for measuring and quantifying physical signals provide an opportunity for the monitoring of physical diseases.

To date, wearable temperature sensors and breath sensors have made great progress in intelligent monitoring. Nevertheless, the external battery is indispensable for most sensors [17–21]. To meet the growing demand of human physiological information monitoring [22,23], some novel pyroelectric sensors have been developed for self-powered human respiratory monitoring. Essentially, polyvinylidene fluoride (PVDF) film has the advantages of flexibility, eco-friendliness and large voltage decay time constant [24–27], which

* Corresponding author (email: 908583913@qq.com, chouxiujian@nuc.edu.cn)
† These authors contributed equally to this work.

presents significant potential for pyroelectric energy harvesting [28] and self-powered sensing [29]. For example, Sun et al. [30] developed a tribo-piezo-pyroelectric composite unit to harvest biomechanical energy and monitor respiratory with a contacting mode. Xue et al. [31] introduced a wearable pyroelectric nanogenerator, examined the integration of a PVDF film in an N95 respirator to harvest the breathing energy of the human body, and demonstrated the function of self-powered breathing sensor. These studies have greatly promoted the development of pyroelectric temperature sensitive unit respiratory monitoring. However, it needs to be connected to the human oral surface, which may cause discomfort. Additionally, piezoelectric [32] and triboelectric [33, 34] sensors are essentially in body contact and not suitable for portable respiratory heat signal monitoring. Currently, there are few reports of real-time and remote physiological information monitoring combined with wireless transmission circuits. As is widely known, an evident difference exists between the breathing gas in the mouth or nose of the human body and surrounding environment (approximately 36°C in oral temperature), particularly in winter. Thus, simultaneous achievement of comfort, portability, mobility, as well as long-distance human heat signal monitoring and transmission is challenging [35].

Herein we proposed a new scheme combining PVDF film and wireless transmission circuit for acquiring human physiological information. The waste heat energy was harvested in a non-contact manner, such as the heat generated from skin, finger, or mouth and nose breathing. Also, the bridge between pyroelectric signals and human physiological signals can be effectively established. The developed sensor shows a fast response time (approximately 400 ms) at a temperature difference of 60 K. Furthermore, an intelligent space heat distribution sensor array integrated with 3×3 units was introduced to track the moving heat source. The sensing system consists of an eco-friendly flexible PVDF pyroelectric sensor and a signal processing circuit, in which the signal processing circuit was assembled with these components like power converter, signal conditioning circuit, data conversion storage module, and wireless Bluetooth data transceiver. The intelligent system can sense the breath heat signal of human mouth or nose in real time and the signal is finally displayed on an Android smartphone terminal. Long-distance (∼10 m) transmission of weak human signals was realized via a signal conditioning circuit. These results indicate that the developed device has potential application in human body temperature and breathing variations monitoring.

2 Experimental section

2.1 Fabrication of PyG sensor and architecture of monitoring system

The fabrication of the pyroelectric generator (PyG) sensor is briefly described as follows. First, the PVDF film with a size corresponding to 3 cm×6 cm×28 μm was cut (purchased from Measurement Specialties). To be used as electrodes, all the Ag layers were connected by wires. The device was then sealed with Kapton tape and pressed with finger pressure to further enhance adhesion between the electrode and functional layer. Finally, the PyG sensor was connected to the test system or a wireless circuit system (Figure 1(a)).

As shown in Figure S1 in Appendix, the power conversion module adopts universal serial bus (USB) to 5 V DC potential, and the regulator chip provides a 3.3 V power supply voltage for the signal conditioning circuit, the main control chip and the wireless Bluetooth module. It ensures the portability and long-term power supply stability of the test system. Secondly, because the output impedance of PyG sensor is very high and the input impedance of wireless Bluetooth circuit is very small, the input resistance of 10 MΩ is selected in the signal conditioning circuit to match with the wireless transmission chip. The heat signal caused by human breathing is a low-frequency signal, usually 0.01–2 Hz. In the signal conditioning circuit, the resistor 680 K and the capacitor 0.1 μF are selected to pass signals with a frequency below 2.3 Hz and reduce external environmental interference. Meanwhile when the heat source periodically approaches and leaves PyG sensor, the periodic oscillating electrical signal was generated. Because half of the oscillating electrical signal is negative values, they cannot be directly used as input signals of the conversion memory module. Therefore, in the signal conditioning module, a level raising circuit with the same direction addition is used to raise the whole output voltage to the positive level, so that the signal conversion memory module can obtain the whole signal. Finally, the signal transmitted to the mobile phone through the Bluetooth module is converted into a positive and negative component of the oscillation signal. Although the signal is not displayed in the original scale, it provides an index for the

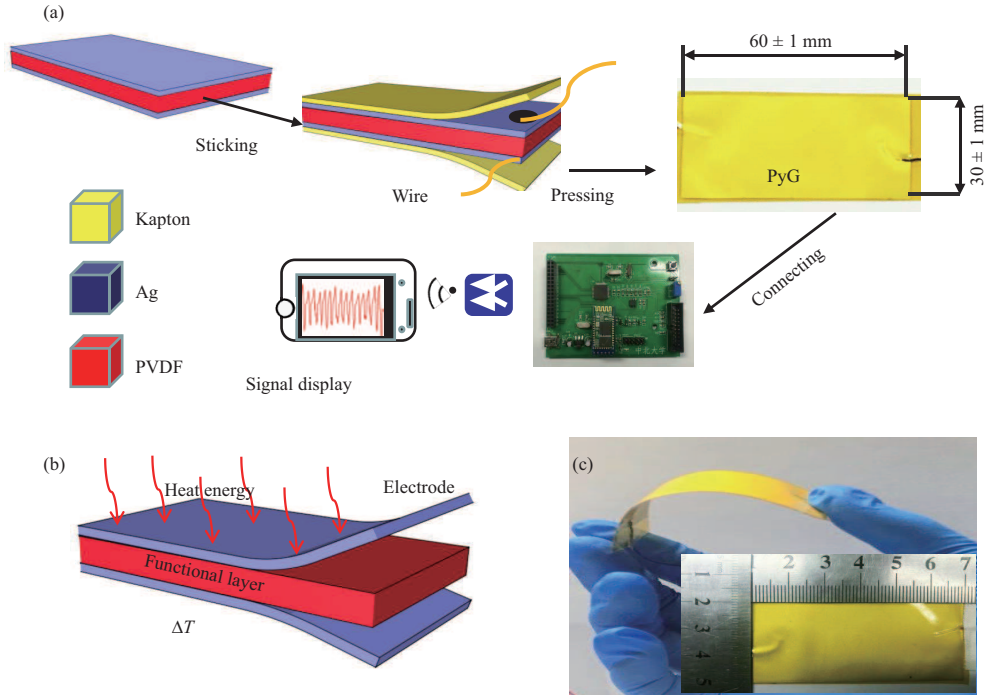

Figure 1 (Color online) (a) Wireless circuit receiving system for pyroelectric signals; (b) capacitance-like structure and thermal radiation heating principle of PyG sensor; (c) photograph of the flexible PyG sensor (the inset shows the dimensions of the PyG sensor).

subsequent practical application of respiratory frequency quantification.

2.2 Device characterization

The PyG sensor was installed in a laboratory with an indoor temperature corresponding to 295 K. A digitally adjustable flexible commercial polyimide heat source (PI) (Wuxi, China) was used to periodically approach and leave the sensor to achieve temperature oscillation on the sensor surface. To make the surface temperature of heat sources more accurate, a K-type thermocouple (TES-1310) was attached to the surface to monitor the temperature of PI heat source in realtime. The output open-circuit voltage and short-circuit current were measured via a Keithley 2611B system electrometer. At the same time, the electrometer was used to collect the voltage output signals of fingers at different pixels of the sensor array. Furthermore, a wireless signal processing circuit, a Bluetooth signal transmission module, and a smartphone APP were used to receive and present signals to monitor the physiological condition of the human body (breathing) in real-time.

3 Results and discussion

3.1 Pyroelectric output of PyG sensor under different ambient heat

As schematically shown in Figure 1(b), PyG sensor has a capacitor-like structure with the pyroelectric crystal as its function layer. To prevent the effect of water vapor on the electrodes the Kapton tape (3 cm×6 cm) was adhered to the flexible PyG device surface. As shown in Figure 1(c), the PyG sensor has light weight characteristics (0.22 g). Evidently, the PyG sensor exhibits good flexibility, indicating its wide application prospects in the field of flexible electronics.

To test the heat-electric conversion of PyG sensor easily and monitor temperature subsequently, the experimental setup is shown in Figure 2(a). Furthermore, the heat source periodically approached and left the sensor to ensure that the output signals were not affected by piezoelectric signals. During the heat source approaching PyG sensor, the distance between them was kept at 1 cm. The temperature variation curve of the heat source is shown in Figure 2(b). The sensor was heated by the heat source for 2 s, and then cooled in the air for 5 s. Figure 2(c) clearly presents the differential curve of the corresponding

temperature change and time of the heat source. In an initial state, the surface temperature of the PyG sensor was close to an indoor temperature of approximately 295 K. Moving the heat source close to PyG sensor for 2 s when its temperature reached 305 K, a positive voltage pulse of approximately 0.37 V can be measured by the test instrument. As the natural convection of the air-cooled slowly for 5 s, the opposite voltage was observed at approximately 0.23 V (Figure 2(d)). It should be noted that the absolute value of the positive pyroelectric output voltage exceeds that of the negative ones. A potential reason for the asymmetrical voltage response phenomenon is that, as shown in Figure 2(b), the temperature change rate of PyG is different under fluctuations in the hot and cold temperature (the maximum temperature change rate of PyG sensor heated by heat source is 6 K/s, while the maximum temperature change rate of PyG sensor cooled by air is 2 K/s).

To investigate the electrical performance of PyG sensor, the comparative experiments with various temperature differences (20, 30, 40, 50, and 60 K) at the relative indoor temperature was set up. As shown in Figure 2(d), the open-voltage values of the PyG sensor evidently increased with the increase of the temperature difference. When the temperature difference was 60 K, the peak-to-peak value of voltage reached the maximum value, which is 12 times when the temperature difference was 10 K. Finally, the maximum positive pyroelectric voltage of PyG sensor at different initial temperatures of the heat source was shown in Figure 2(d). The initial temperature-voltage curve was given in Figure 2(e). And the correlation coefficient (R^2) was 0.9923 for the temperature-voltage curve. The good linearity indicates that it exhibits potential application in self-powered temperature sensing. Additionally, the open-circuit voltage of the PyG sensor on static PI surfaces with different bending radius in the long axis direction was tested to verify its flexible output performance under different curvatures. Meanwhile, the output performance of the fabricated PyG under different bending radii was tested including the bending radius of 20–40 mm in the long axis direction and 20–80 mm in the short axis direction (Figure S2). The results indicate that the positive and negative output voltage pulses were largely unaffected within the radius of curvature range of 35–80 mm in the long axis direction, as displayed in Figure 2(f). More importantly, the results indicated the enormous potential of PyG sensor in temperature sensing or heat-electric conversion on curved surface.

The mechanism underlying the effect of dipole deflection on pyroelectric output has been reported previously [36–38]. The pyroelectric conversion mechanism of PyG is shown in Figure S3. According to the foregoing results and theoretical analysis, the PyG sensor was selected for subsequent testing (including the output voltage and current) at a temperature difference of 60 K under external loading resistances (R_L). As shown in Figure 2(g), the resistance of external load was set in a suitable range of 10^5–10^9 Ω. The results show that the output voltage increases with the increase of load resistance. In the experiments, the low output performance was primarily due to the following factors. First, during the transient process of approaching and leaving the heat source, the heat energy was not completely transferred to the sensor. This is the primary factor affecting the decrease of output performance. It is assumed that the surface temperature of PVDF increased and decreased when the heat source approached and left, respectively. Simultaneously, comsol multi-physics field software was used to simulate its output performance (Figure S4) at a temperature difference of 60 K. A second factor causing the reduction of pyroelectric output was the effect of thermal conductivity between different materials on the overall heat transfer efficiency. Similarly, conversion efficiency of the thermal energy of the PyG sensor was discussed in the supporting information.

As shown in Figure 2(h), the shortcircuit current values exhibit a trend similar to open-circuit voltage values under the same temperature difference. The maximum current value of 75 nA was obtained for the PyG sensor with a 28-μm-thick PVDF film. The inset presents the details of the amplified output current curve. The responding time is approximately 400 ms, laying a foundation for self-powered temperature sensing of the human body or environment.

3.2 Pyroelectric sensor for self-powered breathing or temperature monitoring

Given the preeminent temperature sensitivity of the PyG sensor, it is suitable as a self-powered physiological monitoring device for the human body. For example, the palm or finger temperature can be monitored owing to the temperature difference between the body and environment (while indoor temperature is maintained at 295 K). It is well known that human is warm-blooded. As shown in Figure 3(a), the PyG sensor was driven by the palm repeatedly approaching and leaving. The distance between them was 1 cm when the palm approached PyG sensor. Hence, the periodic voltage signals were measured when

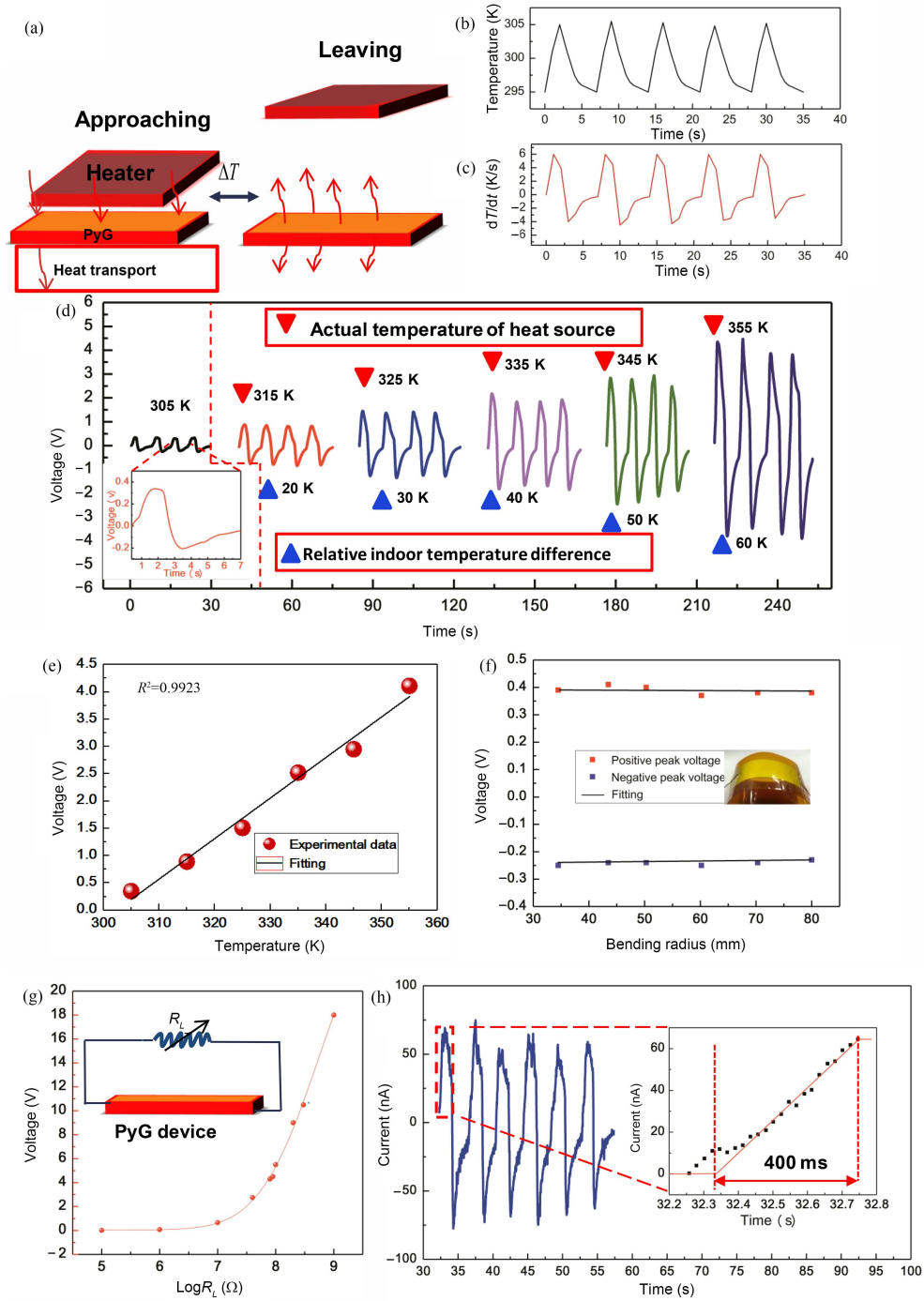

Figure 2 (Color online) (a) Schematic of the experimental setup for the PyG sensor alternately approaching and separating from the heat source. (b) Temperature changes of heat source at an indoor temperature of 295 K. (c) Corresponding temperature variation rate. (d) Output voltage of the PyG sensor under different temperature fluctuations. Inset shows the detailed oscillating voltage of PyG sensor at the cycle temperature in (b). (e) Plot and the linear fit of the open-circuit voltage of the PyG sensor versus the heat flow temperature. (f) Output peak voltage of the PyG sensor on a static curved surface at different bending radius. (g) Dependence of output voltage of PyG sensor on the external loading resistance (inset shows the circuit diagram). (h) Measured short-circuit current of the PyG sensor when the temperature difference between the heat source and the environment was 60 K (inset shows the enlarged output current pulse).

the palm (306 K) repeatedly approached (non-contact) and left the PyG sensor (Figure 3(b)). However, as shown in the figure the experimental output voltages were non-uniform. This was due to the difficulty of controlling the operation precision which should be investigated in future studies. Furthermore, the palm surface temperature was estimated to be approximately 305 K by combining the experiment results

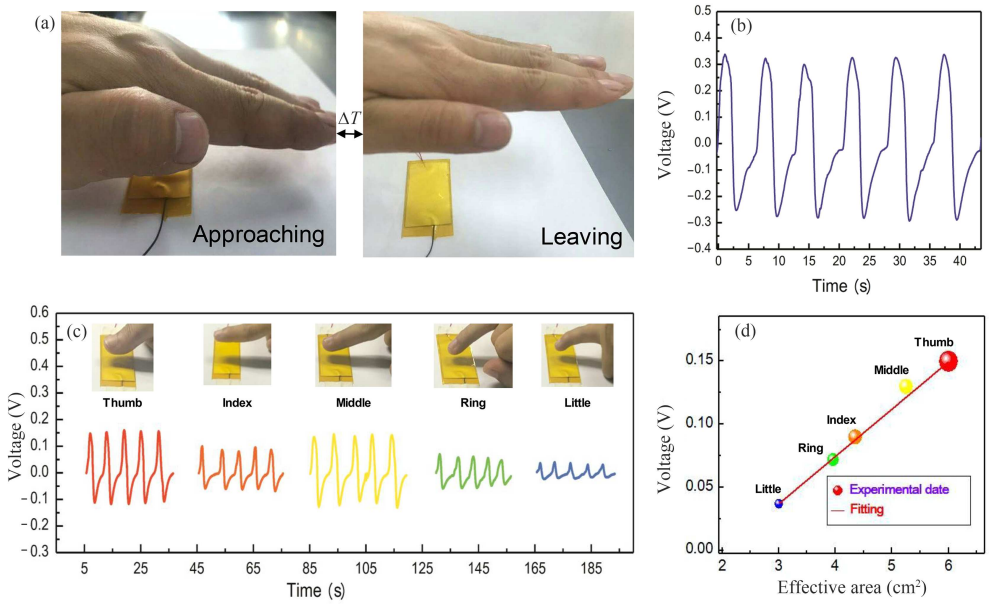

Figure 3 (Color online) (a) Schematic of the PyG sensor driven by the palm. (b) Voltage vs. time curve measured as the palm periodically approached and left the PyG sensor. (c) The output voltage of thumb, index finger, middle finger, ring finger and little finger is close to PyG sensor respectively. (d) Linear fit for different fingers and voltages with respect to PyG sensor effective heating area.

of Figure 2(e) and data in Figure 3(b). Inspired by palm temperature monitoring, the tiny differences in pyroelectric output performance of five different fingers were further measured. The pyroelectric signal amplitude of each finger is accurately monitored (Figure 3(c)), proving the potential application value of PyG sensor in temperature monitoring. With different fingers close to the sensor, the heat affected area is different. The pyroelectric voltage value is proportional to the heating area, and it was well confirmed by five different output signals. When the ambient temperature and finger temperature maintain a certain temperature oscillation, the effective heating area changed. This is a potential reason why the output voltage increased linearly (Figure 3(d)).

Additionally, nose breathing frequency and oral temperature (309.6 K) are extremely important parameters for evaluating human health. Considering the heat exchange via water vapor from mouth or nose breathing with the surrounding environment, generally, the heat energy generated by the water vapor is calculated based on the following equation:

$$M_{\mathrm{PyG}} C_T \Delta T = L m_{\mathrm{H_2O}}, \tag{1}$$

where M_{PyG}, C_T, ΔT, L and $m_{\mathrm{H_2O}}$ denote the mass of the PyG sensor (g), specific heat capacity (1.4 J/gK) [39], temperature variation of the PyG sensor (K) heat delivered to the PVDF (2453.8 J/g at 20°) and water vapor weight (g). According to (1), when the mouth or nose is close to the pyroelectric device, the temperature difference between the PVDF surface and environment is approximately 17 K instantaneously, and the mass of water vapor required is calculated as 2.134 mg. Evidently, water vapor is an important factor that produces a natural temperature difference in the heat exchange between human respiration and the external environment. The PyG sensor breathing device used in an actual indoor environment (295 K) is shown in Figure 4(a) (the distance between the nose and sensor was 1 cm). The open-circuit voltage of the PyG sensor driven by normal nose breathing is shown in Figure 4(b-i). Given its outstanding pyroelectric signal, the device is further used for frequency testing in different breathing states of the human body. Figure 4(b-ii) presents the respiratory rate of the human body (number of breaths per minute) under normal conditions and after running. The output voltage pulse perfectly matches the respiratory rate of the subject in different states, such as normal breathing (13 times per minute) and breathing 19 times per minute after running. It is known that a healthy human body breathes 12–20 times per minute. The foregoing test results are consistent with the respiratory rate of healthy adult. Hence, the PyG sensor can successfully monitor the human respiratory rate. Additionally, the PyG sensor can also be used for monitoring oral temperature in an indoor environment (295 K), as shown in Figure 4(c) (the distance between the mouth and sensor was 1 cm). The amplitudes of the pyroelectric

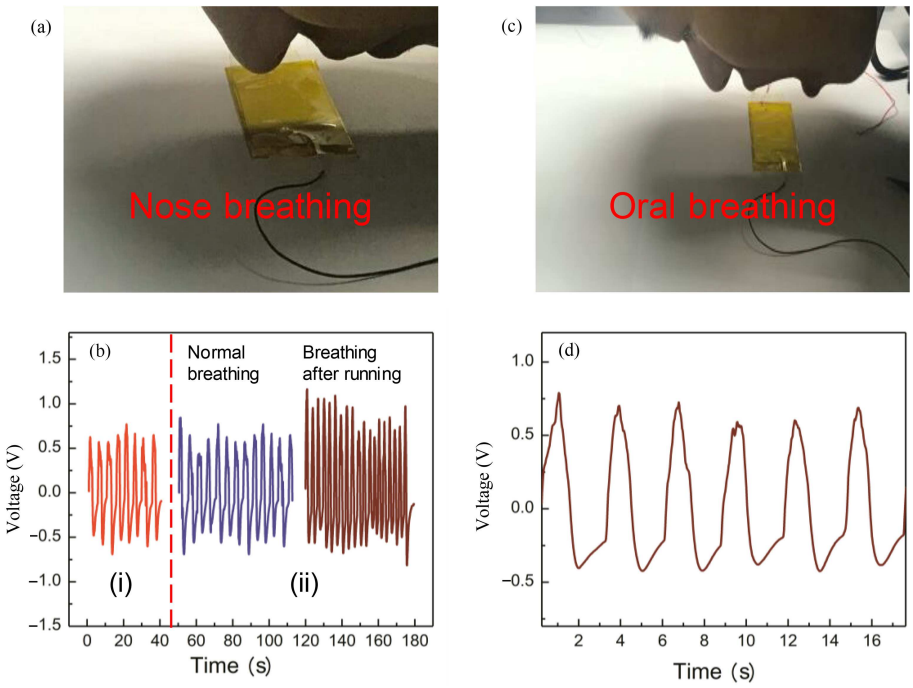

Figure 4 (Color online) (a) Schematic of non-contact PyG sensor driven by human nose breathing. (b-i) The output voltage of the PyG sensor driven by human nose breathing at indoor temperature of 295 K. (b-ii) Respiratory frequency of the human body (number of breaths per minute) after normal breathing and running. (c) Schematic of non-contact PyG sensor driven by human oral breathing. (d) Voltage output of PyG sensor for monitoring oral breathing at indoor temperature of 295 K.

signals for human oral respiration are approximately 0.75 V as indicated by Figure 4(d). Furthermore, combined with the data in Figure 2(e), the oral temperature is estimated to be approximately 309 K. Meanwhile, the long-term repeatability and reliability of the sensors are carried. As shown in Figure S5(a), with the increase of time, when the heat source is set at 305 K (while indoor temperature is maintained at 295 K), the output performance is almost constant after 6 weeks. And the waveform of 104 breaths of the human nose is shown in Figure S5(b). In 480 s, the sensor successfully records the respiratory rate of the human nose, which is 13 breaths per minute (the normal respiratory rate for a healthy adult at rest is 12–18 breaths per minute). Thus, pyroelectric sensors have the function of detecting human health parameters such as respiratory rate and oral temperature, and can monitor human health anytime and anywhere owing to their long-term repeatability and reliability.

Additionally, for more accurate measurement of the spatial temperature distribution to achieve tracking of moving heat sources, a 3×3 sensor array (each approximately 15 mm×15 mm) is prepared. The sensor array was installed in an indoor laboratory (Figure 5(a)). Specifically, "rubbed finger" (RF) indicates that the same initial finger rubs on the palm (Figure 5(b)) for approximately 20 times to heat it up. The output voltages corresponding to the initial finger (302 K) and RF (304 K) approaching different pixel points were demonstrated. Furthermore, the spatial temperature distribution of the finger at different pixel points was obtained, which was attributed to the increase in the surface temperature of finger to 304 K after the physical rubbing stimulation. Additionally, the sensor array can be used as a human-computer interaction interface for finger-movement tracking as shown in Figure 5(c). A finger moved sequentially over the sensor array along the L-path. Figure 5(d) clearly records the finger movement path and can even estimate the finger temperature based on the electrical signal. Compared to single-point or skin thermal imaging tests, the advantage of the sensor array is that it can be dynamically tracked as a non-invasive space heat source.

4 Wireless transmission and display of pyroelectric signals

To gain further insight into the performance of the device for practical real-time personalized health monitoring, the wireless signal processing circuit was designed and integrated with PyG sensor. As shown in Figure 6(a) the wireless printed circuit board (PCB) consists of the following four parts. Part 1

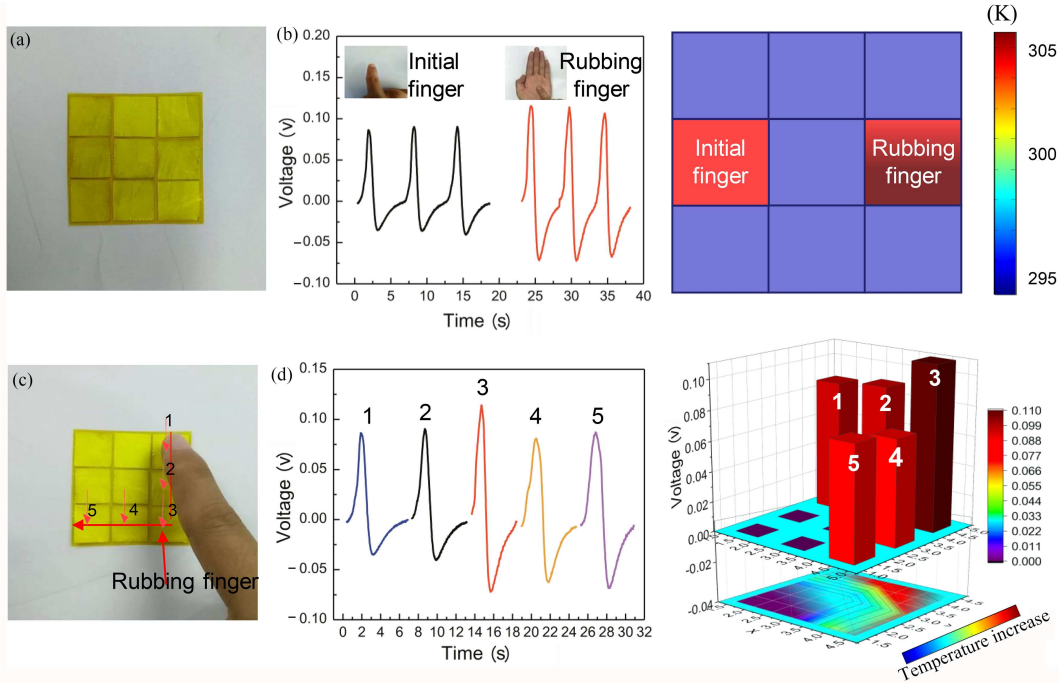

Figure 5 (Color online) (a) Photograph of a 3×3 flexible temperature sensing array. (b) Photograph of output voltages and space temperature distribution corresponding to different pixels. (c) Schematic of finger movement along the path. (d) The corresponding voltage output of the sensor array is used to monitor finger movement.

is a power conversion circuit, Part 2 is a signal conditioning circuit, Part 3 is a conversion storage module between analog signal and digital signal and Part 4 is a wireless Bluetooth data transceiver. The data were ultimately used to evaluate physiological state of the human body and displayed on an Android phone. A detailed flow chart of an integrated system for human physiological signal detection is shown in Figure 6(b). Here, parts 2–4 are connected to a 3.3 V voltage regulator to ensure that they function properly. Subsequently, the human respiratory or oral temperature signals received by the pyroelectric sensor are processed by Part 2 to obtain accurate signals, and the further processed analog signals are converted into digital signals and stored real-time by Part 3. Finally, the cached data are transmitted to the mobile app and displayed by Part 4. Hence, the system simultaneously achieves thermal harvesting and physiological signal monitoring. Figures 6(c) and (d) show wireless detection schematics for oral and nasal breathing signals, respectively. The pyroelectric sensor and wireless PCB were installed on a table or other indoor target where the temperature was set as approximately 295 K. Figure 6(e) shows the display status of the mobile phone interface before testing. The horizontal coordinates represent the time (18 s) of signal acquisition and grid numbers (mV) along the vertical axis indicate the amplitude of the test signal. It is noticed that there is no signal disturbance because the interference signal of the electrical appliance is filtered out by the filter circuit. Figures 6(f) and (g) further illustrate the real-time monitoring results of human exhalation and inhalation process, in which respiratory frequency and oral respiratory signals are presented respectively. Furthermore, the corresponding test video was displayed in real-time (Videos S1 and S2). As indicated by the waveform results at 18 s, the number of breaths is four times, indicating that the human body breaths approximately 14 times per minute. Compared with the pyroelectric voltage of nose breathing 0.55 V, the signal amplitude of human mouth breathing displayed on the mobile phone interface was about 0.75 V. The slight difference indicates the sensitivity of the PVDF film to weak temperature changes and the real-time monitoring ability of wireless sensor system to human mouth breathing and nose breathing. Additionally, owing to the excellent transmission performance of this system, the maximum working range for pyroelectric signal transmission is 10 m (Video S3), which is suitable for real-time monitoring of human rehabilitation in hospitals and personalized household health application equipment. The contrast between our respiratory sensing system and other respiratory equipment was listed in Table 1. Compared with the previously reported, pyroelectric breathing sensors have advantages in operating voltage and response time. At the same time, compared with other self-driven breathing equipment, non-contact measurement solves the

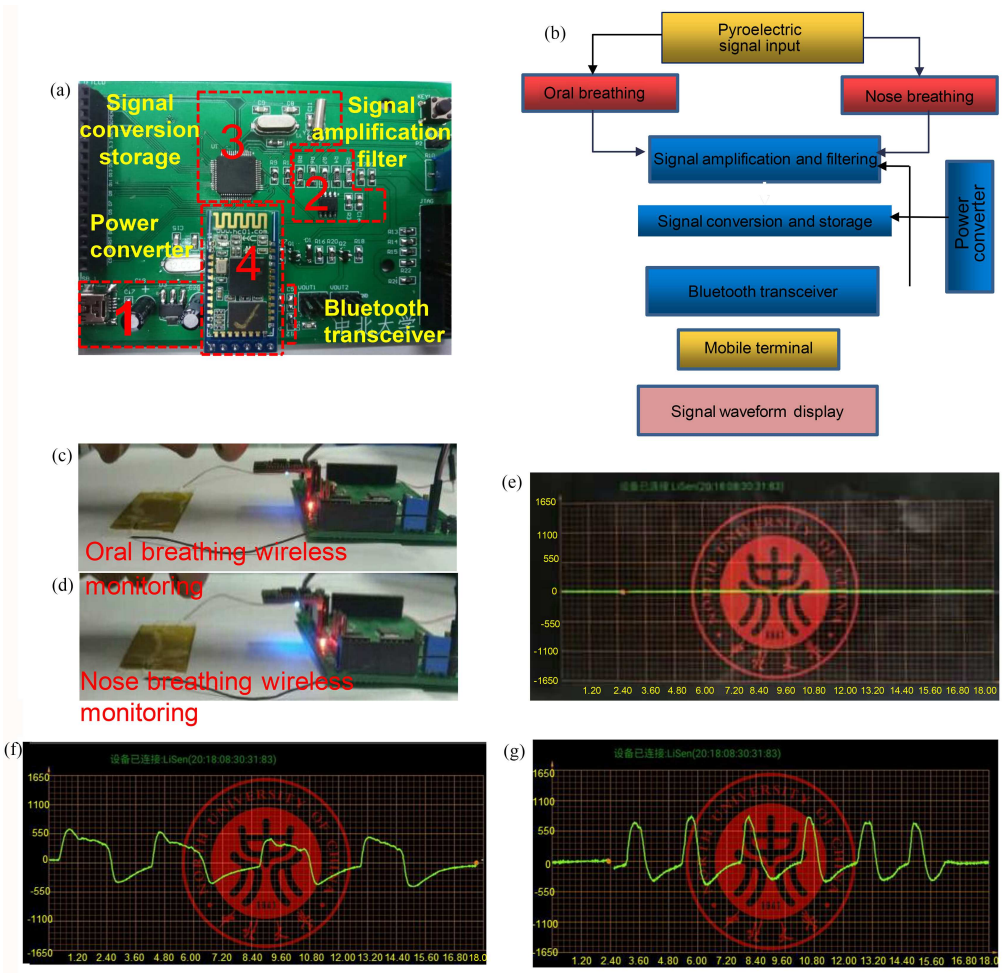

Figure 6 (Color online) (a) Photograph of an integrated system for the wireless PCB. (b) Flow chart of an integrated system for human physiological signal detection. (c) and (d) The schematic of wireless transmission test of human pyroelectric signals. (e) The display status of the mobile phone interface before testing. Real-time display of respiratory signals of the human nose (f) and mouth (g).

Table 1 Summary of partial breathing sensors[a)]

Principle	Sensing material	Wearable/ Non-contact	Monitoring distance	Respone time (s)	Detection range	Operating voltage (V)	Ref.
Pyroelectric	PVDF	Wearable	Short distance	–	5°–25°	Self-driven	[31]
Piezoelectric	PVDF	Wearable	–	–	–	Self-driven	[32]
Triboelectric	Cu/PET	Wearable	–	–	–	Self-driven	[33]
Triboelectric	PTFE/nylon	Wearable	–	0.1	–	Self-driven	[34]
Resistance change	Silica nanoparticles	Wearable	Short distance	0.7	–	9 V	[40]
Resistance change	Graphene oxide	Wearable	Short distance	1.8	12%–97% (RH)	1–5 V	[41]
Resistance change	Polyaniline	Wearable	Short distance	–	54%–98% (RH)	1 V	[42]
Resistance change	Micro-condensation sensor	Non-contact	–	–	–	2.2 V	[43]
Triboelectric	PA6/PVDF	Wearable	–	–	–	Self-driven	[44]
Resistance change	Cellulose paper	Wearable	–	–	0%–90% (RH)	25 V	[45]
Pyroelectric	PVDF	Non-contact	10 m	0.4	295–355 K	Self-driven	This work

a) Abbreviations: polyethylene terephthalate (PET); polytetrafluoroethylene (PTFE); Nylon 6 (PA6).

discomfort of contact measurement, and the long transmission distance solves the non-portability of wired breath monitoring. Meanwhile, pyroelectric sensor has potential application value in human intelligent temperature sensing.

In this study, we sought to demonstrate the universal applicability of wireless sensing systems. Here, in an indoor laboratory, three volunteers were randomly invited to participate in oral and nasal pyroelectric

signal tests, where the temperature was set as approximately 295 K. Figure S6 shows the respiratory and oral signal voltage response values for different volunteers. The signal voltages response values varied slightly among the individual, indicating the difference of participants' breathing rate. This is mainly attributed to factors such as the volunteers' gender and physiological state. Although the testing methods and equipments need to be optimized, our results indicate that the proposed sensing system has the potential of long-term monitoring in personalized human physiological information and has important clinical reference value.

5 Conclusion

In summary, a flexible and portable non-contact highly integrated pyroelectric signal detection system was fabricated which includes a thermally sensitive unit and wireless Bluetooth sensing circuit. In accordance with the heat-electric conversion theory for PVDF film, a maximum peak voltage of 8 V and peak current of 0.15 μA were obtained, respectively, under a temperature difference of 60 K. Compared with conventional temperature sensing, linear output voltage in the temperature range of 295–355 K and fast response time (approximately 400 ms) of PyG sensor exhibit potential for temperature monitoring. The temperature difference between the human body and the surrounding environment makes the signals from human palms, fingers, mouth and nose breathing be successfully captured. On this basis, the 3×3 sensing array was developed for spatial heat distribution monitoring and tracking of moving heat sources. Additionally, human mouth or nose breathing signals can be finally displayed in real-time via an Android phone app. Moreover, the pyroelectric signals can be wirelessly transmitted within a distance of 10 m. This study offers new prospects in the field of rehabilitation and wellness monitoring.

Acknowledgements This work was supported by National Natural Science Foundation of China (Grant Nos. 51705476, 51975542), National Key R&D Project of China (Grant Nos. 2018YFF0300605, 2019YFF0301802), Shanxi "1331 Project" Key Subject Construction (Grant No. 1331KSC), Young Academic Leaders of North University of China (Grant No. QX201805), Program for the Innovative Talents of Higher Education Institutions of Shanxi, and Applied Fundamental Research Program of Shanxi Province (Grant Nos. 201801D221199, 201901D211281). The volunteer who participated in human testing provided informed consent.

Supporting information Figures S1–S6, Table S1, Videos S1–S3. The supporting information is available online at info.scichina.com and link.springer.com. The supporting materials are published as submitted, without typesetting or editing. The responsibility for scientific accuracy and content remains entirely with the authors.

References

1 Lu C F, Wu S, Zhang Y Y, et al. Electromechanical modeling of eye fatigue detecting using flexible piezoelectric sensors. Sci China Inf Sci, 2018, 61: 060417
2 Hu X H, Zhang X, Liu M, et al. A flexible capacitive tactile sensor array with micro structure for robotic application. Sci China Inf Sci, 2014, 57: 120204
3 Han L B, Ding J N, Wang S, et al. Multi-functional stretchable and flexible sensor array to determine the location, shape, and pressure: application in a smart robot. Sci China Tech Sci, 2018, 61: 1137–1143
4 Gao L, Hu D, Qi M, et al. A double-helix-structured triboelectric nanogenerator enhanced with positive charge traps for self-powered temperature sensing and smart-home control systems. Nanoscale, 2018, 10: 19781–19790
5 He J, Wen T, Qian S, et al. Triboelectric-piezoelectric-electromagnetic hybrid nanogenerator for high-efficient vibration energy harvesting and self-powered wireless monitoring system. Nano Energy, 2018, 43: 326–339
6 Strauß R, Ewig S, Richter K, et al. The prognostic significance of respiratory rate in patients with pneumonia: a retrospective analysis of data from 705928 hospitalized patients in Germany from 2010–2012. Deutsches Aerzteblatt Online, 2014, 111: 503–508
7 Trung T Q, Lee N E. Flexible and stretchable physical sensor integrated platforms for wearable human-activity monitoringand personal healthcare. Adv Mater, 2016, 28: 4338–4372
8 Webb R C, Bonifas A P, Behnaz A, et al. Ultrathin conformal devices for precise and continuous thermal characterization of human skin. Nat Mater, 2013, 12: 938–944
9 Yokota T, Inoue Y, Terakawa Y, et al. Ultraflexible, large-area, physiological temperature sensors for multipoint measurements. Proc Natl Acad Sci USA, 2015, 112: 14533–14538
10 Guo W, Tan C, Shi K, et al. Wireless piezoelectric devices based on electrospun PVDF/BaTiO3 NW nanocomposite fibers for human motion monitoring. Nanoscale, 2018, 10: 17751–17760
11 He X, Zi Y, Yu H, et al. An ultrathin paper-based self-powered system for portable electronics and wireless human-machine interaction. Nano Energy, 2017, 39: 328–336
12 Jeon J, Lee H B R, Bao Z. Flexible wireless temperature sensors based on Ni microparticle-filled binary polymer composites. Adv Mater, 2013, 25: 850–855
13 Li Q, Zhang L N, Tao X M, et al. Review of flexible temperature sensing networks for wearable physiological monitoring. Adv Healthcare Mater, 2017, 6: 1601371
14 Youn D Y, Jung U, Naqi M, et al. Wireless real-time temperature monitoring of blood packages: silver nanowire-embedded flexible temperature sensors. ACS Appl Mater Interfaces, 2018, 10: 44678–44685

15 Pereira C B, Yu X, Czaplik M, et al. Estimation of breathing rate in thermal imaging videos: a pilot study on healthy human subjects. J Clin Monit Comput, 2017, 31: 1241–1254
16 Li W, Liang T, Liu W, et al. Wireless passive pressure sensor based on sapphire direct bonding for harsh environments. Sens Actuat A-Phys, 2018, 280: 406–412
17 Chen W, Liu P, Liu Y, et al. A temperature-induced conductive coating via layer-by-layer assembly of functionalized graphene oxide and carbon nanotubes for a flexible, adjustable response time flame sensor. Chem Eng J, 2018, 353: 115–125
18 Tai Y, Chen T, Lubineau G. A sandwiched/cracked flexible film for multithermal monitoring and switching devices. ACS Appl Mater Interfaces, 2017, 9: 32184–32191
19 Hong S Y, Lee Y H, Park H, et al. Stretchable active matrix temperature sensor array of polyaniline nanofibers for electronic skin. Adv Mater, 2016, 28: 930–935
20 Liu Q, Tai H, Yuan Z, et al. A high-performances flexible temperature sensor composed of polyethyleneimine/reduced graphene oxide bilayer for real-time monitoring. Adv Mater Technol, 2019, 4: 1800594
21 Ren X, Pei K, Peng B, et al. A low-operating-power and flexible active-matrix organic-transistor temperature-sensor array. Adv Mater, 2016, 28: 4832–4838
22 Yu J, Hou X, Cui M, et al. Highly skin-conformal wearable tactile sensor based on piezoelectric-enhanced triboelectric nanogenerator. Nano Energy, 2019, 64: 103923
23 Yu J, Hou X, He J, et al. Ultra-flexible and high-sensitive triboelectric nanogenerator as electronic skin for self-powered human physiological signal monitoring. Nano Energy, 2020, 69: 104437
24 Ebrahim S, Elshaer A M, Soliman M, et al. Pyroelectric infrared detector based on polyaniline/polyvinylidene fluoride blend. Sens Actuat A-Phys, 2016, 238: 389–396
25 Wu Q, Li X, Yang X, et al. Pyroelectric infrared device with overlap dual capacitor structure sensor. Sens Actuat A-Phys, 2018, 282: 192–196
26 Zi Y, Lin L, Wang J, et al. Triboelectric-pyroelectric-piezoelectric hybrid cell for high-efficiency energy-harvesting and self-powered sensing. Adv Mater, 2015, 27: 2340–2347
27 You M H, Wang X X, Yan X, et al. A self-powered flexible hybrid piezoelectric-pyroelectric nanogenerator based on non-woven nanofiber membranes. J Mater Chem A, 2018, 6: 3500–3509
28 Leng Q, Chen L, Guo H, et al. Harvesting heat energy from hot/cold water with a pyroelectric generator. J Mater Chem A, 2014, 2: 11940–11947
29 Zhang H, Xie Y, Li X, et al. Flexible pyroelectric generators for scavenging ambient thermal energy and as self-powered thermosensors. Energy, 2016, 101: 202–210
30 Sun J G, Yang T N, Wang C Y, et al. A flexible transparent one-structure tribo-piezo-pyroelectric hybrid energy generator based on bio-inspired silver nanowires network for biomechanical energy harvesting and physiological monitoring. Nano Energy, 2018, 48: 383–390
31 Xue H, Yang Q, Wang D, et al. A wearable pyroelectric nanogenerator and self-powered breathing sensor. Nano Energy, 2017, 38: 147–154
32 Mahbub I, Pullano S A, Wang H, et al. A low-power wireless piezoelectric sensor-based respiration monitoring system realized in CMOS process. IEEE Sens J, 2017, 17: 1858–1864
33 Zhang B, Tang Y, Dai R, et al. Breath-based human-machine interaction system using triboelectric nanogenerator. Nano Energy, 2019, 64: 103953
34 Zhang H, Zhang J, Hu Z, et al. Waist-wearable wireless respiration sensor based on triboelectric effect. Nano Energy, 2019, 59: 75–83
35 Liu H, Allen J, Zheng D, et al. Recent development of respiratory rate measurement technologies. Physiol Meas, 2019, 40: 07TR01
36 Yang Y, Jung J H, Yun B K, et al. Flexible pyroelectric nanogenerators using a composite structure of lead-free KNbO(3) nanowires. Adv Mater, 2012, 24: 5357–5362
37 Tien N T, Seol Y G, Dao L H A, et al. Utilizing highly crystalline pyroelectric material as functional gate dielectric in organic thin-film transistors. Adv Mater, 2009, 21: 910–915
38 Lang S B. Pyroelectricity: from ancient curiosity to modern imaging tool. Phys Today, 2005, 58: 31–36
39 Cuadras A, Gasulla M, Ferrari V. Thermal energy harvesting through pyroelectricity. Sens Actuat A-Phys, 2010, 158: 132–139
40 Kano S, Dobashi Y, Fujii M. Silica nanoparticle-based portable respiration sensor for analysis of respiration rate, pattern, and phase during exercise. IEEE Sens Lett, 2018, 2: 1–4
41 Pang Y, Jian J, Tu T, et al. Wearable humidity sensor based on porous graphene network for respiration monitoring. Biosens Bioelectron, 2018, 116: 123–129
42 Lv R, Li S, Jin T, et al. Hybrid core-shell nanofibers as moisture sensors for human breath monitoring. Compos Sci Tech, 2018, 162: 58–63
43 Janik P, Pielka M, Janik M A, et al. Respiratory monitoring system using Bluetooth low energy. Sens Actuat A-Phys, 2019, 286: 152–162
44 Qiu H J, Song W Z, Wang X X, et al. A calibration-free self-powered sensor for vital sign monitoring and finger tap communication based on wearable triboelectric nanogenerator. Nano Energy, 2019, 58: 536–542
45 Güder F, Ainla A, Redston J, et al. Paper-based electrical respiration sensor. Angew Chem Int Ed, 2016, 55: 5727–5732